# The Greenland Ice-Marginal Lake Inventory Series from 2016 to 2023

Penelope How<sup>1</sup>, Dorthe Petersen<sup>2</sup>, Kristian K. Kjeldsen<sup>1</sup>, Katrine Raundrup<sup>3</sup>, Nanna B. Karlsson<sup>1</sup>, Alexandra Messerli<sup>2</sup>, Anja Rutishauser<sup>1</sup>, Jonathan L. Carrivick<sup>4</sup>, James M. Lea<sup>5</sup>, Robert S. Fausto<sup>1</sup>, Andreas P. Ahlstrøm<sup>1</sup>, and Signe B. Andersen<sup>1</sup>

**Correspondence:** Penelope How (pho@geus.dk)

Abstract. The Greenland Ice Sheet and its surrounding peripheral glaciers and ice caps (PGICs) are projected to be the largest cryospheric contributor to sea level rise this century. While glacial meltwater is typically assumed to flow directly into the ocean, ice-marginal lakes temporarily store a portion of this runoff, influencing glacier dynamics and ablation, ecosystems, and downstream hydrology. Their presence, and change in abundance and size, remain under-represented in projections of sea level change and glacier mass loss. Here, we present an eight-year (2016–2023) inventory of 2918 automatically classified ice-marginal lakes (>=0.05 km<sup>2</sup>) across Greenland, tracking changes in lake abundance, surface extent, and summer surface temperature over time. Fluctuations in lake abundance were most pronounced at the north (22%) and northeast (14%) PGIC margins and the southwest Ice Sheet margin (8%). Over the study period, an increase in surface lake area was evident at 243 lakes, a decreasing trend was evident at 675 lakes, and 778 lakes remained stable (± 0.05 km<sup>2</sup>). The northeast region contained the largest lakes, averaging 1.63 km<sup>2</sup> at the ice sheet margin and 1.58 km<sup>2</sup> at PGIC margins. Water surface temperatures fluctuated between 3.8 °C (2018) and 5.3 °C (2023), with spatial and temporal trends identified with possible links to lake setting and size. Validation against manually identified lakes showed 64% agreement, yielding an error estimate of  $\pm$  809 lakes (36%), while lake extent uncertainty was  $\pm$  0.77 km<sup>2</sup>. Surface temperature estimates showed strong agreement with in situ measurements ( $r^2 = 0.87$ , RMSE = 1.68 °C, error  $\pm$  1.2 °C). This dataset provides a crucial foundation for quantifying meltwater storage at ice margins and refining sea level contribution projections while supporting research on glacier-lake interactions, Arctic ecology, and environmental management. The inventory series is openly accessible on the GEUS Dataverse (https://doi.org/10.22008/FK2/MBKW9N) with full metadata, documentation, and a reproducible processing workflow (How et al., 2025).

# 1 Introduction

The Greenland Ice Sheet and its peripheral glaciers and ice caps (PGICs) are forecast to be the largest cryospheric contributor to sea level rise over the coming century (Arctic Monitoring and Assessment Programme (AMAP), 2021). At present, these

<sup>&</sup>lt;sup>1</sup>Department of Glaciology and Climate, Geological Survey of Denmark and Greenland, Denmark

<sup>&</sup>lt;sup>2</sup>Department of Hydrology and Climate, Asiag Greenland Survey, Greenland

<sup>&</sup>lt;sup>3</sup>Department of Environment and Mineral Resources, Greenland Institute of Natural Resources, Greenland

<sup>&</sup>lt;sup>4</sup>School of Geography and water@leeds, University of Leeds, UK

<sup>&</sup>lt;sup>5</sup>Department of Geography and Planning, University of Liverpool, UK

projections assume that meltwater from the Greenland Ice Sheet flows directly into the ocean, yet a portion of this is known to be stored temporarily in ice-marginal lakes, along the ice edge of the Greenland Ice Sheet and in front of and beside surrounding PGICs. The delayed release of meltwater at the ice margin is a significant, dynamic component of terrestrial storage, as well as a substantial CO<sub>2</sub> sink and part of the hydrological system (St. Pierre et al., 2019). Ice-marginal lakes around the Greenland Ice Sheet form as meltwater becomes trapped at the terminus or edges of an outlet glacier (How et al., 2021; Carrivick et al., 2022). Many of these lakes can be persistent and stable (Carrivick and Quincey, 2014), but an increasing number are recognised to be highly dynamic systems (Dømgaard et al., 2024). For example, many ice-marginal lakes are prone to sudden and short-lived drainage events, thereby producing GLOFs (Glacial Lake Outburst Flood events) (e.g., Taylor et al., 2023) which are also referred to as *jökulhlaups* (Icelandic) (e.g., Eibl et al., 2023) or *sermimit supinerit* (direct translation into Kalaallisut, West Greenlandic; in singular *sermimit supineq*) (Oqaasileriffik, personal communication, November 2024). GLOFs in Greenland can have characteristics of megafloods (Carrivick and Tweed, 2019) and have caused glacier speed-up events (e.g., Kjeldsen et al., 2017), influenced downstream erosion and sedimentation rates (e.g., Carrivick et al., 2013; Tomczyk et al., 2020), and water salinity (e.g., Grinsted et al., 2017; Kjeldsen et al., 2014).

The presence of an ice-marginal lake introduces a suite of thermo-mechanical processes, including lacustrine submarine melting and calving, that can dictate glacier margin morphology, dynamics and exacerbate ice mass loss (Warren and Kirkbride, 2003; Röhl, 2006; Carrivick and Tweed, 2019; Sutherland et al., 2020; Zhang et al., 2023b). With continued retreat of the Greenland Ice Sheet under a warming climate, ice-marginal lakes and their associated processes are expected to become more abundant, larger, and warmer, which will likely amplify lacustrine-driven proglacial melt rates and GLOF events (Carrivick and Tweed, 2016; Grinsted et al., 2017; Shugar et al., 2020; Carrivick et al., 2022; Dye et al., 2021; Dømgaard et al., 2023; Lützow et al., 2023; Rick et al., 2023; Veh et al., 2023; Holt et al., 2024; Zhang et al., 2024). However, ice-marginal lakes and their associated processes are largely absent from sea level change projections, which assume an immediate meltwater contribution to the ocean. This assumption overlooks the role of ice-marginal lakes as intermediary storage, and changes in lacustrine and hydrological conditions, caused for instance when glaciers retreat onto land.

35

45

55

Mapping ice-marginal lakes is challenging due to the variability in lake characteristics. Remote sensing has been a viable approach for mapping the presence and surface extent of ice-marginal lakes, as demonstrated by inventories in Greenland (How et al., 2021), Alaska (Rick et al., 2022), Norway (Andreassen et al., 2022), Svalbard (Wieczorek et al., 2023) and High Mountain Asia (Chen et al., 2021). In general, classification approaches have been established to identify water bodies from SAR (Synthetic Aperture Radar) and multi-spectral (i.e. red, green, blue, near-infrared, shortwave) imagery, along with water potential identification using sink analysis from Digital Elevation Models (DEMs). As Greenland covers a large latitudinal range, ice-marginal lakes have very varying conditions which make them difficult to classify through one adopted method (How et al., 2021). For instance, surface sediment load, ice, and snow cover can vary significantly, with perennial ice cover in some cases at high latitudes and elevations (e.g., Mallalieu et al., 2021). Accordingly, multi-method classification approaches are necessary to capture this diversity (How et al., 2021).

Existing ice-marginal lake inventories are often static and therefore do not capture the dynamic nature of these lakes, nor capture new lakes and retire detached lakes once the margin has retreated. Given that ice-marginal lakes are projected to

increase in size and abundance over time (Shugar et al., 2020; Zhang et al., 2024), it is of utmost importance to generate time-series that adequately capture ice-marginal lake change and could potentially contribute to future sea level assessments.

Here, we present an annual series of Greenland ice-marginal lakes from 2016 to 2023, classified using an established multimethod remote sensing approach. Each annual inventory maps the number of lakes (i.e. abundance) and lake surface area, along with attributes such as known lake name and water surface temperature estimations. These inventories reveal evolving lake conditions that support future assessments of sea level contribution, lake response to climate change, ecosystem productivity, and biological activity associated with the Greenland Ice Sheet and the PGICs.

# 2 Data description

#### 2.1 Dataset overview

65

70

The Greenland ice-marginal lake annual inventory series is a follow-on from the 2017 Greenland ice-marginal lake inventory, largely adopting the same classification approach, data structure and formatting (How et al., 2021). How et al. (2021) provided the first Greenland-wide ice-marginal lake inventory as a static dataset, building upon regional multi-temporal efforts, such as the southwest inventory classified from Landsat imagery (Carrivick and Quincey, 2014).

The dataset presented consists of a series of annual inventories, mapping the presence and extent of ice-marginal lakes across Greenland (Figure 1). Ice-marginal lakes are defined as water bodies > 0.05 km<sup>2</sup> (based on satellite image spatial resolution), which are immediately adjacent to (and therefore in contact with) the Greenland Ice Sheet and/or the PGICs of Greenland. The annual inventory series spans the entirety of Greenland, including all terrestrial regions. Thus far, there are 8 annual inventories, covering the Sentinel satellite era from 2016 to 2023, where one inventory represents one year.

# 75 2.2 Data sources and acquisition

Ice-marginal lakes are identified using three established classification methods, from Synthetic Aperture Radar (SAR) and multi-spectral imagery, and Digital Elevation Models (DEMs). Classifications from SAR and multi-spectral imagery for each inventory year are identified from all available Sentinel-1 and Sentinel-2 image acquisitions for the months of July and August (Table 1). DEM classifications are made from a static data product which covers the period 2008 to 2016. Metadata for each identified lake includes a lake surface temperature estimate, which is derived from Landsat 8/9 thermal band imagery (Table 1).

# 2.3 Data format and structure

The inventory series data are distributed as polygon vector features in an open GeoPackage format (.gpkg), with coordinates provided in the WGS NSIDC Sea Ice Polar Stereographic North (EPSG:3413) projected coordinate system. File names follow the convention defined in the original 2017 Greenland ice-marginal lake inventory (Wiesmann et al., 2021; How et al., 2021): <inventory-year>-<funder>-cinventory-year>-<funder>--cinventory-year>-<funder>--cinventory-year>-<funder>-

Table 1. Summary of satellite data sources

Satellite	Data product	Acquisition filters	Spatial resolution
Sentinel-1	Ground Range Detected (GRD) dual-	Interferometric Wide Swath (IW),	10 metres
	polarization C-band SAR images	Horizontal-Horizontal (HH) polarisa-	
		tion, 01 Jul to 31 Aug	
Sentinel-2	Multispectral instrument (MSI), Top of	01 Jul to 31 Aug, 20% max. cloud cover	10 metres
	Atmosphere (TOA), Level 1C images		
-	ArcticDEM mosaic (version 3)	-	2 metres
Landsat 8/9	Operational Land Imager/Thermal In-	01 to 31 Aug, 20% max. cloud cover	100 metres
	frared Sensor (OLI/TIRS), Collection		
	2, Level 2, surface temperature science		
	product		

Each GeoPackage file contains metadata regarding the lake description, physical measurements, lake surface temperature, method/s of classification, verification and possible editing (Table 2). A key piece of metadata to highlight is the lake identification number ("lake\_id", Table 2), which are assigned to each classified ice-marginal lake, often consisting of multiple polygon features and/or classifications. These unique identifications are compatible across inventory years, therefore supporting timeseries analysis and comparison across inventories.

Information is included regarding whether the adjacent ice margin is either the ice sheet or PGIC ("margin", Table 2). This margin information originates from the MEaSUREs GIMP 15 m ice mask, previously used for the spatial filtering. In addition, each ice-marginal lake is assigned a region – north-west (NW), north (NO), north-east (NE), central-east (CE), south-east (SE), south-west (SW), and central-west (CW) ("region", Table 2). These regions and their corresponding names are based on ice sheet catchment regions from Mouginot and Rignot (2019), which are used to also extend to the terrestrial periphery beyond the ice sheet. By doing so, regional trends can be identified from ice-marginal lakes with a PGIC margin as well as the ice sheet (Carrivick et al., 2022).

Lake names ("lake\_name", Table 2) are assigned in instances where a name is available, with preference to West Greenlandic (Kalaallisut) placenames followed by Old Greenlandic and alternative foreign placenames. Placenames are provided by Oqaasileriffik (the Language Secretariat of Greenland) placename database (https://nunataqqi.gl/), filtering placenames to those associated with lake features. The placename database is distributed with QGreenland v3.0 (Moon et al., 2023).

A readme file is included with the dataset that outlines the data file contents and terms of use. An additional data file is included which is a point vector GeoPackage file representing all identified lakes across the inventory series (presented in Figure 1). This includes manually identified lake locations that are not captured in the inventory series using the automated classification approaches.

# 3 Methodology

#### 3.1 Lake classification

Lake classifications (>=0.05 km²) were based on those adopted in the production of the 2017 Greenland ice-marginal lake inventory, which is summarised in Figure 2 (How et al., 2021). The main progression (and therefore difference) is that the processing pipeline is now unified and operates through Google Earth Engine to conduct the heavy image processing (How, 2024), and filtering/post-processing conducted with open-source spatial packages in Python, namely geopandas (Kelsey et al., 2020) and rasterio (Gillies et al., 2013–). The Python pipeline is deployable as a package called GrIML (How, 2024), which is accompanied by thorough documentation and guidelines (https://griml.readthedocs.io). This ensures a high level of reproducibility and transparency that adheres to the FAIR (Findability, Accessibility, Interoperability, and Reusability) principles (Wilkinson et al., 2016).

# 3.1.1 SAR backscatter classification

Water bodies were classified from Sentinel-1 GRD scenes, which are dual-polarization C-band SAR images (Table 1). Scenes were pre-processed using the Sentinel-1 Toolbox to generate calibrated, ortho-corrected data, specifically thermal noise removal, radiometric calibration and terrain correction using either the SRTM 30 or ASTER DEM. Scenes were then filtered to IW swath and HH polarisation, with image acquisitions limited to the summer months (1 July to 31 August) of each inventory year (2016 to 2023). Averaged mosaics for each year were derived from all summer scenes for each year of the inventory series at a 10 m spatial resolution. These mosaics were smoothed using a focal median of 50 metres. Classifications were derived from these averaged and smoothed mosaics using a static threshold trained for detecting open water bodies (How et al., 2021).

# 125 3.1.2 Multi-spectral indices classification

130

135

Water bodies were classified from Sentinel-2 MSI, TOA, Level-1C scenes acquired for the summer months (1 July to 31 August) of each inventory year (2016 to 2023) (Table 1). Clouds were masked using the cloud mask provided with each scene (QA60), masking out opaque and cirrus clouds. The bands of interest were extracted, specifically blue (B2), green (B3), red (B4), near-infrared (B8), and the two shortwave infrared bands (B11, B12) (Table 3). The shortwave infrared bands were resampled from 60 m to 10 m spatial resolution, and then averaged band mosaics were produced from all summer scenes for each inventory year.

Five spectral indices were used to classify open water bodies: 1) Normalised Difference Water Index (McFeeters, 1996); 2) Modified Normalised Difference Water Index (Xu, 2006); 3) Automated Water Extraction Index (with shadow) (Feyisa et al., 2014); 4) Automated Water Extraction Index (no shadow) (Feyisa et al., 2014); 5) Snow brightness radio (How et al., 2021) (Table 3). The thresholds for the indices were chosen based on previous studies of ice-marginal lakes (How et al., 2021; Shugar et al., 2020), where positive classifications adhered to all thresholds.

# 3.1.3 Sink classification

155

160

165

Water bodies were classified from the ArcticDEM 2-metre mosaic (version 3), which is compiled from the best quality ArcticDEM strip files and manually adjusted to form a static data product (Porter et al., 2018). The mosaic was smoothed using a focal median of 110 metres, and DEM depressions (i.e. where water pools) were filled over a 50-pixel moving window and subsequently subtracted from the original mosaic; producing the outline of a lake (Table 1). It is noted that this is an indirect water classification method compared to the former two approaches (which directly detect water). Therefore, validation was required to confirm the presence of water in classified DEM sinks, which will be elaborated further in the following subsection.

# 3.2 Summer water surface temperature estimation

A summer water surface temperature estimate was provided for each classified lake across inventory years. Water surface temperature estimates were derived from the Landsat 8 and Landsat 9 OLI/TIRS surface temperature data, which is a Collection 2, Level-2 science product that is part of a large Landsat re-processing effort (Table 1). Surface temperature estimates were generated from descending, day-lit Landsat 8/9 acquisitions with thermal infrared band information (100 metre spatial resolution) and auxiliary data (i.e. Top Of Atmosphere reflectance and brightness temperature), along with ASTER datasets (global emissivity and normalised difference vegetation index) and MODIS and VIIRS atmospheric auxiliary data (geopotential height, specific humidity and air temperature) (Earth Resources Observation and Science (EROS) Center, 2020; Malakar et al., 2018; U.S. Geological Survey, 2023).

Due to the lack of in situ lake surface temperature measurements in Greenland, the scheme proposed by Dyba et al. (2022) was adopted, whereby surface temperature values ( $LST_{land}$ ) were corrected to water surface temperature ( $LST_{water}$ ) using the following calibration:

$$LST_{scaled} = LST_{land} \times 0.00341802 + 149.0$$
 (1)

$$LST_{water} = (0.806 \times LST_{scaled} + 54.37) - 273.15 \tag{2}$$

Where  $LST_{scaled}$  is the applied scale factor for computing temperature in Kelvin (K) units, and  $LST_{water}$  is the calibrated water surface temperature in degrees Celsius (Ermida et al., 2020; NASA Applied Remote Sensing Training (ARSET) program, 2022; Dyba et al., 2022). This calibration has previously shown strong correlations against in situ measurements (average RMSE = 2.8 °C and  $R^2$  = 0.8) from 38 lakes in Poland, highlighting accurate estimates through a simple linear calibration (Dyba et al., 2022). Ideally, a correction factor specifically for calibrating values to Greenland lakes would be adopted. However, in situ validation datasets in Greenland are sparse and the derived correction factor appears to agree well with the limited datasets available. In the future, more in situ observations would strengthen the assessment, with a possibility to derive a Greenland-specific correction scheme.

A summer average water surface temperature estimate was derived using this approach for each lake extent in the ice-marginal lake inventory series. Scenes were filtered by a maximum cloud cover of 20%, with acquisitions limited to the month of August to reduce the probability of ice-covered lake conditions. Lake extents were cropped by a border pixel (i.e. 100

metres) to reduce the impact of edge effects, and all unrealistic estimates below freezing (i.e. < 0 °C) were removed. An average, maximum and minimum water surface temperature value was computed for each lake extent over each inventory year, along with the standard deviation.

# 4 Results

175

185

# 4.1 Lake abundance

In total, the dataset identifies 2918 automatically delineated ice-marginal lakes across all inventory years (2016-2023) (Figure 1). Of these lakes, 2054 share a margin with the ice sheet whilst 864 are in contact with PGICs (Figure 3). The SW region holds the most lakes compared to other regions, with 786 classifications (640 classified at the ice sheet margin and 146 at the PGIC margins). A high abundance of PGIC lakes is found in the NO region, with 278 lakes, compared to only 37 PGIC lakes in SE. This reflects the presence of more PGICs in northern Greenland, compared to the greater ice sheet cover in the southeast.

Small fluctuations in the abundance of lakes are evident, fluctuating between 1963 (inventory year 2021) and 1827 (inventory year 2022) lakes (Figure 3). The largest variation in lake abundance at the ice sheet is evident at the SW margin, with a fluctuating range of 48 lakes (8%) between 567 (2018, 2023) and 615 lakes (2021) (Figure 3a). The CW and SE margin experienced the least variability, only varying by 16 lakes and 15 lakes, respectively. Changes in lake abundance at the ice sheet margin do not follow any spatial or temporal trends, with fluctuations unconnected to inventory year or margin region.

Lakes at the margins of periphery ice caps and glaciers vary between 723 (inventory year 2022) and 806 (inventory year 2019), with an average range of 11 lakes at the margins of periphery ice caps and glaciers (compared to an average range of 26 lakes at the ice sheet margin) (Figure 3b). The largest fluctuations in lake abundance are seen in the NO and NE regions, fluctuating by 22 (8%) and 29 lakes (14%), respectively. This is linked to the higher number of lakes in these regions, which is supported by the smallest fluctuations evident in the regions where fewer lakes are present (i.e. NW, SE, CE and CW).

#### 4.2 Lake surface extent

The largest lake in the inventory is Romer Sø, located in northeast Greenland, with a total area of 126.86 km² (Figure 1). The average lake size is 1.29 km², and the median lake size is 0.27 km² with 2395 lakes between 0.05-1.00 km² (82%). Only 59 lakes in the inventory series have a total area above 10 km² (2%). The NE and SW regions hold the largest lakes on average, with an average lake area of 1.63 km² (median: 0.34 km²) and 1.58 km² (median: 0.27 km²), respectively. On average, the largest PGIC lakes are also located in the NE region (1.43 km²), likely because Romer Sø skews the PGIC average for this region.

The inventory series also holds information on the change in lake area over time, by comparing corresponding lake extents from each inventory year classified using a direct classification method (i.e. from SAR and/or multi-spectral imagery) (Figure 3). Change in average lake area over the ice sheet margin is relatively consistent across the inventory series, with the smallest change evident at the CE ice sheet margin (0.30 km<sup>2</sup>) and the largest change evident at the NO ice sheet margin (1.31 km<sup>2</sup>)

200 (Figure 3a). Average lake size is highest in the NE region in 2018 and 2022, with an average size of 2.71 km<sup>2</sup> and 2.77 km<sup>2</sup>, respectively; coinciding with the lowest lake abundance. The average lake area is smaller across Greenland's PGIC margins, with an average lake area of 1.00 km<sup>2</sup>, compared to lakes adjacent to the ice sheet with an average lake area of 1.40 km<sup>2</sup> (Figure 3b). Fluctuations in the average lake area across the inventory series are generally much smaller, apart from in the CE and NE regions which range across 2.20 km<sup>2</sup> and 1.76 km<sup>2</sup>, respectively.

Overall, lake area change trends can be tracked at 918 lakes in the inventory series (31% of all mapped lakes), with 243 experiencing growth between 2016 and 2023 (i.e. an increase in area of > 0.05 km<sup>2</sup>), 675 declining in size (i.e. a decrease in area of > 0.05 km<sup>2</sup>) and 778 remaining the same size (i.e. a change in lake area limited to  $\pm$  0.05 km<sup>2</sup>) (Figure 4). The largest lake area changes are experienced at the larger lakes generally, such as those found in the NE region (Figure 4b) and the SW region (Figure 4d).

The inventory series demonstrates changes to lake morphology (and the corresponding change in ice margin morphology), of which four example scenarios are presented in Figure 5. A classic terminus basin retreat style is evident across many ice-marginal lake extents, as presented in Figure 5a, where terminus retreat/lake expansion is marked in the central section of the glacier outlet, leaving a trailing terminus morphology at the lateral margins. Peripheral terminus retreat is highlighted in Figure 5b, where terminus retreat/lake expansion is focused at the lateral margins. There are instances where the presence of a lake affects the boundary conditions of two glacier termini, as demonstrated in Figure 5c, where two glaciers terminate into the same common ice-marginal lake. And finally, there are instances displayed in the inventory series where there is margin retreat/lake expansion focused around a discrete zone, such as in Figure 5d where a marked embayment has formed at a particular point in the north region of the glacier terminus.

# 4.3 Lake surface temperature

205

An average surface temperature estimate was derived for each inventory lake from all available Landsat 8/9 scenes acquired in the month of August for each inventory year (see Section 3.2). This information is provided in the metadata of the ice-marginal lake inventory series. Examining the average lake surface temperature estimate across all lakes (i.e. the sum of all lake averages divided by the number of lakes), the average lake surface temperature fluctuates between 3.8 °C (2018) and 5.3 °C (2023) (Figure 6). Fluctuations year on year vary, with instances of lake temperature being lower between annual time steps (e.g. from 4.5 °C to 3.8 °C from 2017 to 2018), higher (e.g. from 4.8 °C to 5.3 °C from 2022 to 2023), and remaining consistent (e.g. 4.8 °C for 2021 to 2022).

Average surface temperature can be examined spatially across each lake in the inventory series (Figure 7a). This reveals an apparent latitudinal trend, with lakes across the northern regions (NO, NW, and NE) being cooler, on average, than those in the southern regions (SW, SE). The northern regions have a higher abundance of lakes with an average surface temperature between 0 and 4 °C, whereas lake temperature in the southern regions tends to be between 4 and 10 °C. There are visible exceptions to this spatial trend, such as ice-marginal lakes present in nunatak areas which are generally cooler because of a greater presence of ice surrounding them and/or beneath them.

When assessing lake temperature through time, lake size appears to influence the average surface temperature and the rate of temperature change across each inventory year (Figure 7b). The smallest lakes (<= 0.1 km<sup>2</sup>) are warmest, on average, with an average temperature of 5.45 °C and the overall average varying between 4.9 and 5.9 °C. The largest lakes (5.0-150.0 km<sup>2</sup>) are colder, with an average temperature of 3.9 °C, varying between 3.5 and 4.5 °C. Lakes with a smaller surface extent (<= 0.5 km<sup>2</sup>) remained relatively consistent temperatures across each inventory year, with the average fluctuating by a maximum of 0.2 °C between 2016 and 2023 °C (Figure 7b). The largest lakes in the inventory series (5.0-150.0 km<sup>2</sup>) experienced the largest temperature change between 2016 and 2023, cooling by an average of 0.5 °C.

# 240 5 Data quality and validation

235

250

255

260

## 5.1 Data quality control

Identified water bodies were compiled for each inventory year and filtered via three strategies: 1) by location; 2) by size; 3) by manual curation (Figure 2). Firstly, lakes were filtered based on their location relative to the ice margin. Here, a 1 km buffer was derived around the MEaSUREs GIMP 15 m ice mask and classified water bodies were retained if they were located within the buffer (Howat, 2017; Howat et al., 2014). Classified water bodies were filtered by size, only retaining lakes above a minimum size threshold of 0.05 km² based on the spatial resolution of the source satellite imagery; as adopted by How et al. (2021). Finally, each inventory year dataset was manually curated to remove misclassifications, edit classifications (for example, where the shadowing mask did not adequately remove shadowing effects), remove detected water bodies that did not hold water in specific years, and remove water bodies that were detached from the ice margin. This manual curation was carried out via visual inspection of Sentinel-2 TOA Level-1C true colour composites from each inventory year.

Classification information is provided with the ice-marginal lake inventory series, so that the performance of each classification method can be evaluated (Figure 8). 14,020 of all detections in the inventory series (66%) were classified using only one of the methods, composed largely from the DEM method (Figure 8a). 5156 detections were classified using two methods (24%), and 2264 detections were classified using all three methods (11%). It is noted that the number of classification methods is not a measure of certainty but instead should be interpreted as a reflection of lake appearance and its adherence to the criteria of each classification method, as well as satellite data availability.

The SW region was typically where most lakes were classified with all three classification methods; across both the ice sheet margin (Figure 8b) and the PGIC margins (Figure 8c). This is likely because the classification methods have been extensively applied and developed in the SW region compared to others (e.g., Carrivick and Quincey, 2014; Carrivick et al., 2017; Kjeldsen et al., 2017). The DEM method was heavily relied upon in the NO and NE regions where direct classification of open water was challenging as lakes were more likely to be consistently ice/snow covered, and satellite image availability from Sentinel-1 and Sentinel-2 was limited (How et al., 2021).

# 5.2 Lake abundance error estimation

265

270

280

285

290

Previous error analysis suggested that the 2017 ice-marginal lake inventory captured 92% of lake abundance, based on comparison between the inventory and user-defined lakes over four regions at the NE, NW and SW ice sheet margin, and a region within the PGICs, covering a collective area of  $40,000 \text{ km}^2$ . This formed an error estimate for lake abundance of  $\pm$  8% (see How et al. (2021) for more details). As a follow-on to this effort, ice-marginal lakes were manually verified for each inventory year, including those that were not classified using the automated methods. Across all inventory years, 4543 ice-marginal lakes were manually identified in total, of which 2915 (64%) are present in the ice-marginal lake inventory series. This forms a revised lake abundance error estimation of  $\pm$  809 (36%). This error estimation is substantially different from the former estimate because the 2017 ice-marginal lake inventory included manual lake delineations, whereas the inventory series presented here only includes automated classifications (i.e. no manual lake delineations are included).

# 5.3 Lake size error estimation

Lakes classified with both the SAR backscatter and multi-spectral indices classification approaches were compared to assess variability in footprint size and provide an error estimation of lake extent. Classifications with the sink detection approach were excluded from this analysis, as the sink detection approach is an indirect measurement of lake extent rather than a direct classification of water. Across all ice-marginal lake classifications within the inventory series, 3070 lakes were successfully classified with both the SAR backscatter and multi-spectral indices classification approaches. On average, there is a difference of 1.54 km<sup>2</sup> between the two classifications, with a median difference of 0.17 km<sup>2</sup>. An error estimate of  $\pm$  0.77 km<sup>2</sup>, should therefore be adopted as an error estimate for classified lake extents.

## 5.4 Lake surface temperature error estimation

Water surface temperature estimates were validated against all known and/or open-access in situ measurements of lake temperature in Greenland (Figure 9). The only continuous/long-term in situ surface measurements (i.e. <= 2 m) are from six lake records in southwest Greenland - Kangerluarsunnguup Tasia (64°07'50"N, 51°21'36"W) and Qassi-Sø (64°09'14"N, 51°18'27"W) (Greenland Ecosystem Monitoring, 2024), Russell Lake (67°13'77"N, 50°07'63"W) (courtesy of Kristian K. Kjeldsen), and three lakes as part of the Asiaq Greenland Survey hydrological monitoring programme (Qassi-Sø 2024 measurements; Qamanersuaq, 63°47'71"N, 50°00'50"W; and an unnamed lake referred to as Asiaq station 924, 64°12'99"N, 51°36'39"W).

Comparison of the 133 coinciding in situ measurements with those estimated using the remote sensing approach adopted here exhibit a strong correlation ( $r^2 = 0.87$ ), with an RMSE of 1.68 °C, suggesting that the remotely sensed temperature estimates are reliable (Figure 9). This trend appears to be consistent regardless of the time of year. An interesting cluster of data points is evident, originating from measurements taken at Qamanersuaq and Asiaq station 924 which could be related to specific lake characteristics, such as lake depth/morphology or suspended sediment concentration. An error estimation of  $\pm$  1.2 °C is determined, based on the average difference from data points across all lake sites.

# 6 Potential applications and future updates

295

300

305

310

315

320

325

# 6.1 Uses for the ice-marginal lake inventory series

The inventory series presented here is the first step to quantifying the terrestrial storage of meltwater, and how it changes over time, which would be highly valuable for refining estimations of the future sea level contribution of the Greenland Ice Sheet and surrounding PGICs. Tentative findings have been outlined, yet further analysis and evaluation against other datasets is needed to investigate causal links. For example, the inventory series could be used to address the drivers of change in lake area with comparison to potential influences such as meltwater flux, sedimentation rates, bedrock type, and GLOF magnitude and frequency (e.g. Veh et al., 2025). The inventory series could also be incorporated with mapping efforts of terrestrial lakes (i.e. no contact with the ice margin) to provide a detailed overview of dynamic and stable storage of water at the terrestrial margins of Greenland (e.g Danish Climate Data Agency, 2025). Additionally, the inventory series would be a valuable dataset for examining lacustrine terminus retreat dynamics, expanding investigations from a case study basis (e.g. Mallalieu et al., 2021; Langhamer et al., 2024) to a regional and/or national scale (e.g. Dye et al., 2022).

The ice-marginal lake inventory series is applicable to climate and cryosphere research, enabling inter-annual comparison of lake change (abundance, extent and surface temperature) over time, similar to inventories for other regions such as Svalbard (Wieczorek et al., 2023). Such inventories have been used to characterise ice dam types (e.g., Rick et al., 2022), monitor GLOFs (e.g., Lützow et al., 2023), and assess lake conditions in catchments of interest (e.g., Hansen et al., In Press). Lake conditions could also provide insights into glacier dynamics in lacustrine settings around Greenland, for example, to investigate submarine melting in lacustrine settings and its impact on glacier retreat (e.g., Mallalieu et al., 2021). More widely, the lake changes documented in this inventory series would be valuable to studies of the redistribution of mass on the earth surface, affecting gravity, geodesy and lithospheric elastic response (e.g., Ran et al., 2024).

Beyond scientific research, the inventory series will also be a useful resource in Greenland's assessment of infrastructure, with hydropower being the main sector that could benefit. Given Greenland's commitment to the Paris Agreement strongly suggests the expansion of current hydropower infrastructure, the ice-marginal lake inventory series could be valuable in infrastructure assessments (Naalakkersuisut, 2023). For example, the inventory series can be used to distinguish glacier-fed lakes from catchment-fed lakes, identify draining lakes, and other characteristics that are useful to discern viable catchment regions.

#### 6.2 The future of the ice-marginal lake inventory series

It is planned to update the ice-marginal lake inventory series annually with new inventory years, using the methodology and data sources outlined here. Further automated classification methods need to be explored and incorporated into the data production pipeline to address the under detection of ice-marginal lakes, as highlighted in the validation of automated classifications against manual detections (see Section 5.2). Methodologies such as Forel-Ule color indexing (FUI) have been successfully applied to the detection of lakes in the High Arctic (Urbański, 2022), and more widely in a global context (Wang et al., 2021), which could be suitable for applying to ice-marginal lakes in Greenland after testing their accuracy and feasibility. Another avenue to explore is the inclusion of manually delineated lake extents where lakes have not been identified with the

automated classification approaches. However, this would add further labour to the manual curation of the inventory series. An alternative would be to look at implementing new automated classification methods with machine learning, using the existing lake classifications as the foundation of a training dataset. Lake classification aided by machine learning has been successfully used for supraglacial lake detection on the Greenland Ice Sheet, so the use of machine learning in ice-marginal lake detection is likely to be feasible (Lutz et al., 2023; Melling et al., 2024).

One of the key limitations of this work to be addressed in the future is the reliance on static data products, in particular the static ArcticDEM 2 m mosaic for classification, and the MEaSURES GIMP static ice margin for filtering. The use of static data products in the inventory series presented here highlights the importance of high-labour, time-consuming manual dataset curation. For the DEM classification, an alternative would be SAR-derived DEMs from the TanDEM-X mission or the ArcticDEM strip data product, which are both time variant, but data coverage is lacking currently and scenes covering all Greenland may not be possible from year to year (e.g., Lutz et al., 2024). Another option would be to use coarser spatial resolution DEM products, such as PRODEM (500 m) (Winstrup et al., 2024), however, smaller lakes would not be identifiable. For the ice margin filtering, machine learning ice margin products show promise in being used in future editions of the inventory series, such as AutoTerm (trained with the TeamPicks dataset) (Goliber et al., 2022; Zhang et al., 2023a). The use of dynamic ice margin datasets in the future could negate the need for generating a classification spatial buffer around the margin data and instead classify ice-marginal lakes directly from their intersection with the ice margin position.

Another opportunity for future iterations of the inventory series could be to include past years, prior to the Sentinel satellite era. However, this is limited by the open availability of SAR and multi-spectral satellite imagery at a high spatial resolution (i.e. 10 metres). The addition of valuable metadata could also be explored, including information such as the characteristics and dynamics of each classified ice-marginal lake. The type of damming has been included in other inventories, proving to be useful for assessing present and future lake conditions under a changing climate (e.g., Rick et al., 2022). Incorporating known GLOFs and/or drainage periods for each lake would also provide insight into abrupt changes in terrestrial water storage and be highly valuable information for infrastructure assessments, such as hydropower utilities (e.g., Dømgaard et al., 2024).

# 7 Conclusions

330

335

340

350

355

Here, a series of annual inventories is presented that represent ice-marginal lake abundance, surface area extents, and surface temperature estimates across Greenland for the years 2016 to 2023. Ice-marginal lakes are mapped across the margin of the Greenland Ice Sheet and its surrounding PGICs. The dataset demonstrates lake change over the 8-year period, which can be assessed at various scales, from individual lake, to regional, to Greenland-wide change. The annual ice-marginal lake inventory series is openly available on the GEUS Dataverse with a cite-able DOI at https://doi.org/10.22008/FK2/MBKW9N (How et al., 2025) and an open, reproducible workflow (How, 2024).

The dataset reveals small fluctuations in the abundance of lakes year on year, with the largest variations occurring at the NO (22%) and NE (14%) PGIC margins, and the SW Ice Sheet margin (8%). The NE region holds the largest lakes, with an average lake area of 1.63 km<sup>2</sup> at the ice sheet margin and 1.58 km<sup>2</sup> at the PGIC margins (including Romer Sø, the largest lake

in the inventory series). Between 2016 and 2023, 243 lakes grew in size, 675 shrank in size and 778 remained the same size ( $\pm$  0.05 km<sup>2</sup>). A summer surface temperature estimate is provided for each lake across the inventory series, demonstrating an average temperature fluctuation between 4.3 °C (2018) and 5.9 °C (2023) and evident spatial and temporal trends influenced by lake setting and size.

The ice-marginal lake inventory series was validated against manually identified lakes to assess its accuracy in lake abundance, revealing that 64% of manual identifications are adequately captured in the inventory series. This formed an error estimate of  $\pm$  809 lakes (36%). SAR backscatter and multi-spectral indices classifications were compared to assess the uncertainty in detected lake extent, providing an error estimate of  $\pm$  0.77 km<sup>2</sup>. Lake surface temperature estimates were compared against existing in situ surface (<= 2 m) lake measurements from Greenland, exhibiting a strong correlation (r<sup>2</sup> = 0.87; RMSE = 1.68 °C) and an error estimate of  $\pm$  1.2 °C.

The annual ice-marginal lake inventory series is a valuable addition to addressing current limitations in terrestrial water storage and its influence on Greenland's future sea level contribution. This dataset is the first step towards quantifying meltwater storage at the margins of the Greenland Ice Sheet, and surrounding PGICs. It also provides insight into lake change over time, and the resulting impact on glacier dynamics, such as lacustrine frontal ablation (i.e. submarine melting and calving). Beyond the cryospheric science community, the dataset will be invaluable to related disciplines in biology and ecology, where changes in lake conditions shape Arctic ecosystems and biological activity. On a national level, the inventory series could be a useful resource in environmental management and infrastructure assessment, for instance in the expansion of hydropower utilities as suggested in Greenland's new commitments to the Paris Agreement.

# 8 Code and data availability

365

375

The dataset is openly available on the GEUS Dataverse at https://doi.org/10.22008/FK2/MBKW9N (How et al., 2025), distributed under a CC BY 4.0 license (https://creativecommons.org/licenses/by/4.0/). If the dataset is presented or used to support results of any kind then we ask that a reference to the dataset be included in publications, along with any relevant publications from the data production team. If the dataset is crucial to the main findings, we encourage users to reach out to the authorship team as this will likely improve the quality of the work that uses this product. The production code for making the inventory series is openly available at https://github.com/GEUS-Glaciology-and-Climate/GrIML (How, 2024). It is distributed as a deployable and version-controlled Python package. If the production code is used or adapted, then we ask for a reference to be included in publications.

Author contributions. P.H. led the production workflow and dataset presented, with input from D.P., K.K.K., N.B.K., A.M., A.R., J.L.C. and J.M.L. Validation datasets were collected and curated by D.P., K.K.K. and K.R. Management of the project and work presented was overseen by R.S.F., A.P.A. and S.B.A. All authors contributed to the manuscript text.

Competing interests. The authors declare that there are no competing interests.

395

400

Acknowledgements. P.H. was supported by an ESA (European Space Agency) Living Planet Fellowship (4000136382/21/I-DT-Ir) entitled "Examining Greenland's Ice Marginal Lakes under a Changing Climate (GrIML)". Further support was provided by the Programme for Monitoring of the Greenland Ice Sheet (PROMICE), funded by the Geological Survey of Denmark and Greenland (GEUS) and the Danish Ministry of Climate, Energy and Utilities under the Danish Cooperation for Environment in the Arctic (DANCEA), conducted in collaboration with DTU Space (Technical University of Denmark) and Asiaq Greenland Survey. The ArcticDEM mosaic used in this study is provided by the Polar Geospatial Center under NSF-OPP awards 1043681, 1559691, 1542736, 1810976, and 2129685. In situ lake temperature datasets are supported by the GrIML project (with measurement collection led by Asiaq Greenland Survey), BioBasis under the Greenland Ecosystem Monitoring Programme (GEM), and the Greenland Integrated Observing System (GIOS) under the Danish Agency for Higher Education and Science. K.K.K. acknowledges support from the Independent Research Fund in Denmark (grant ID 10.46540/3103-00234B). J.M.L. acknowledges support from his UK Research and Innovation (UKRI) Future Leaders Fellowship (MR/X02346X/1). Additional thanks to Stephen Plummer and Marcus Engdahl for technical advice and support, and Sikkersoq Olsen and Arnaq Brandt Johansen from Oqaasilerif-fik (the Language Secretariat of Greenland) for clarification on the Kalaallisut terminology for GLOFs.

# References

- Andreassen, L. M., Nagy, T., Kjøllmoen, B., and Leigh, J. R.: An inventory of Norway's glaciers and ice-marginal lakes from 2018–19 Sentinel-2 data, Journal of Glaciology, 68, 1085–1106, https://doi.org/10.1017/jog.2022.20, 2022.
  - Arctic Monitoring and Assessment Programme (AMAP): Arctic Climate Change Update 2021: Key Trends and Impacts. Summary for Policy-makers, Arctic Monitoring and Assessment Programme (AMAP), Tromsø, Norway, 16 pp, 2021.
- Carrivick, J. L. and Quincey, D. J.: Progressive increase in number and volume of ice-marginal lakes on the western margin of the Greenland

  Ice Sheet, Global and Planetary Change, 116, 156–163, 2014.
  - Carrivick, J. L. and Tweed, F. S.: A global assessment of the societal impacts of glacier outburst floods, Global and Planetary Change, 144, 1–16, https://doi.org/10.1016/j.gloplacha.2016.07.001, 2016.
  - Carrivick, J. L. and Tweed, F. S.: A review of glacier outburst floods in Iceland and Greenland with a megafloods perspective, Earth-Science Reviews, 196, 102 876, https://doi.org/10.1016/j.earscirev.2019.102876, 2019.
- 415 Carrivick, J. L., Turner, A. G. D., Russell, A. J., Ingeman-Nielsen, T., and Yde, J. C.: Outburst flood evolution at Russell Glacier, western Greenland: effects of a bedrock channel cascade with intermediary lakes, Quaternary Science Reviews, 67, 39–58, https://doi.org/10.1016/j.quascirev.2013.01.023, 2013.
  - Carrivick, J. L., Tweed, F. S., Ng, F., Quincey, D. J., Mallalieu, J., Ingeman-Nielsen, T., Mikkelsen, A. B., Palmer, S. J., Yde, J. C., Homer, R., Russell, A. J., and Hubbard, A.: Ice-Dammed Lake Drainage Evolution at Russell Glacier, West Greenland, Frontiers in Earth Science, 5, 100, https://doi.org/10.3389/feart.2017.00100, 2017.
  - Carrivick, J. L., How, P., Lea, J. M., Sutherland, J. L., Grimes, M., Tweed, F. S., Cornford, S., Quincey, D. J., and Mallalieu, J.: Ice-Marginal Proglacial Lakes Across Greenland: Present Status and a Possible Future, Geophysical Research Letters, 49, e2022GL099276, https://doi.org/10.1029/2022GL099276, 2022.
- Chen, F., Zhang, M., Guo, H., Allen, S., Kargel, J. S., Haritashya, U. K., and Watson, C.: Annual 30 m dataset for glacial lakes in High Mountain Asia from 2008 to 2017, Earth System Science Data, 13, 741–766, https://doi.org/10.5194/essd-13-741-2021, 2021.
  - Danish Climate Data Agency: Dataforsyningen: Åbent Land Grønland, Databoks Grønland, https://dataforsyningen.dk/data/4771, 2025.
  - Dømgaard, M., Kjeldsen, K. K., Huiban, F., Carrivick, J. L., Khan, S. A., and Bjørk, A. A.: Recent changes in drainage route and outburst magnitude of the Russell Glacier ice-dammed lake, West Greenland, The Cryosphere, 17, 1373–1387, https://doi.org/10.5194/tc-17-1373-2023, 2023.
- Dømgaard, M., Kjeldsen, K., How, P., and Bjørk, A.: Altimetry-based ice-marginal lake water level changes in Greenland, Communications Earth and Environment, 5, 365, https://doi.org/10.1038/s43247-024-01522-4, 2024.
  - Dyba, K., Ermida, S., Ptak, M., Piekarczyk, J., and Sojka, M.: Evaluation of Methods for Estimating Lake Surface Water Temperature Using Landsat 8, Remote Sensing, 14, 3839, https://doi.org/10.3390/rs14153839, 2022.
- Dye, A., Bryant, R., Doff, E., Falcini, F., and Rippin, D. M.: Warm Arctic Proglacial Lakes in the ASTER Surface Temperature Product,
  Remote Sensing, 13, 2987, https://doi.org/10.3390/rs13152987, 2021.
  - Dye, A., Bryant, R., and Rippin, D.: Proglacial lake expansion and glacier retreat in Arctic Sweden, Geografiska Annaler: Series A, Physical Geography, 104, 268–287, https://doi.org/10.1080/04353676.2022.2121999, 2022.
  - Earth Resources Observation and Science (EROS) Center: Landsat 8-9 Operational Land Imager / Thermal Infrared Sensor Level-2, Collection 2 [dataset], U.S. Geological Survey, https://doi.org/10.5066/P9OGBGM6, 2020.

- Eibl, E. P. S., Vogfjörd, K. S., Ófeigsson, B. G., Roberts, M. J., Bean, C. J., Jones, M. T., Bergsson, B. H., Heimann, S., , and Dietrich, T.: Subaerial and subglacial seismic characteristics of the largest measured jökulhlaup from the eastern Skaftá cauldron, Iceland, Earth Surface Dynamics, 11, 933–959, https://doi.org/10.5194/esurf-11-933-2023, 2023.
  - Ermida, S. L., Soares, P., Mantas, V., Göttsche, F.-M., and Trigo, I. F.: Google Earth Engine Open-Source Code for Land Surface Temperature Estimation from the Landsat Series, Remote Sensing, 12, 1471, https://doi.org/10.3390/rs12091471, 2020.
- Feyisa, G. L., Meilby, H., Fensholt, R., and Proud, S. R.: Automated Water Extraction Index: A new technique for surface water mapping using Landsat imagery, Remote Sensing of Environment, 140, 23–35, https://doi.org/10.1016/j.rse.2013.08.029, 2014.
  - Gillies, S. et al.: Rasterio: geospatial raster I/O for Python programmers, Mapbox, https://github.com/rasterio/rasterio, 2013-.
  - Goliber, S., Black, T., Catania, G., Lea, J. M., Olsen, H., Cheng, D., Bevan, S., Bjørk, A., Bunce, C., Brough, S., Carr, J., Cowton, T., Gardner, A., Fahrner, D., Hill, E., Joughin, I., Korsgaard, N. J., Luckman, A., Moon, T., Murray, T., Sole, A., Wood, M., , and Zhang,
- E.: TermPicks: a century of Greenland glacier terminus data for use in scientific and machine learning applications, The Cryosphere, 16, 3215–3233, https://doi.org/10.5194/tc-16-3215-2022, 2022.
  - Greenland Ecosystem Monitoring: BioBasis Nuuk Lakes Temperature in lakes (Version 1.0). [Data set] [CC-BY-SA-4.0], Greenland Ecosystem Monitoring, https://doi.org/10.17897/BKTY-J070, 2024.
- Grinsted, A., Hvidberg, C. S., Campos, N., and Dahl-Jensen, D.: Periodic outburst floods from an ice-dammed lake in East Greenland,

  Scientific Reports, 7, 9966, https://doi.org/10.1038/s41598-017-07960-9, 2017.
  - Hansen, K., Karlsson, N. B., How, P., Poulsen, E., Mortensen, J., and Rysgaard, S.: Winter subglacial meltwater detected in Greenland Fjord, Nature Geosciences, In Press.
  - Holt, E., Nienow, P., and Medina-Lopez, E.: Terminus thinning drives recent acceleration of a Greenlandic lake-terminating outlet glacier, Journal of Glaciology, pp. 1–13, https://doi.org/10.1017/jog.2024.30, 2024.
- 460 How, P.: PennyHow/GrIML v0.1.0, Zenodo, https://doi.org/10.5281/zenodo.11395471, 2024.
  - How, P., Messerli, A., Mätzler, E., Santoro, M., Wiesmann, A., Caduff, R., Langley, K., Bojesen, M. H., Paul, F., Kääb, A., and Carrivick, J. L.: Greenland-wide inventory of ice marginal lakes using a multi-method approach, Scientific Reports, 11, 4481, https://doi.org/10.1038/s41598-021-83509-1, 2021.
- How, P., Petersen, D., Karlsson, N. B., Kjeldsen, K. K., Raundrup, K., Messerli, A., Rutishauser, A., Carrivick, J. L., Lea, J. M., Fausto, R. S.,
   Ahlstrøm, A. P., and Andersen, S. B.: Greenland Ice Marginal Lake Inventory annual time-series Edition 1 [dataset], GEUS Dataverse,
   https://doi.org/10.22008/FK2/MBKW9N, 2025.
  - Howat, I.: MEaSUREs Greenland Ice Mapping Project (GIMP) land ice and ocean classification mask, version 1 [GimpIce-Mask 15 m tiles 0-5], NASA National Snow and Ice Data Center Distributed Active Archive Center, Boulder, Colorado USA, https://doi.org/10.5067/B8X58MQBFUPA, 2017.
- Howat, I. M., Negrete, A., and Smith, B. E.: The Greenland Ice Mapping Project (GIMP) land classification and surface elevation data sets, Cryosphere, 8, 1509–1518, https://doi.org/10.5194/tc-8-1509-2014, 2014.
  - Kelsey, J. et al.: geopandas/geopandas: v0.8.1, Zenodo, https://doi.org/10.5281/zenodo.394676, 2020.
  - Kjeldsen, K. K., Mortensen, J., Bendtsen, J., Petersen, D., Lennert, K., and Rysgaard, S.: Ice-dammed lake drainage cools and raises surface salinities in a tidewater outlet glacier fjord, west Greenland, Journal of Geophysical Research: Earth Surface, 119, 1310–1321,
- 475 https://doi.org/10.1002/2013JF003034, 2014.

- Kjeldsen, K. K., Khan, S. A., Bjørk, A. A., Nielsen, K., and Mouginot, J.: Ice-dammed lake drainage in west Greenland: Drainage pattern and implications on ice flow and bedrock motion, Geophysical Research Letters, 44, 7320–7327, https://doi.org/10.1002/2017GL074081, 2017.
- Langhamer, L., Sauter, T., Temme, F., Werner, N., Heinze, F., Arigony-Neto, J., Gonzalez, I., Jaña, R., and Schneider, C.: Response of lacustrine glacier dynamics to atmospheric forcing in the Cordillera Darwin, Journal of Glaciology, 70, e8, https://doi.org/10.1017/jog.2024.14, 2024.
  - Lutz, K., Bahrami, Z., and Braun, M.: Supraglacial Lake Evolution over Northeast Greenland Using Deep Learning Methods, Remote Sensing, 15, 4360, https://doi.org/10.3390/rs15174360, 2023.
- Lutz, K., Bever, L., Sommer, C., Seehaus, T., Humbert, A., Scheinert, M., and Braun, M.: Assessing supraglacial lake depth using ICESat-2, Sentinel-2, TanDEM-X, and in situ sonar measurements over Northeast and Southwest Greenland, The Cryosphere, 18, 5431–5449, https://doi.org/10.5194/tc-18-5431-2024, 2024.
  - Lützow, N., Veh, G., and Korup, O.: A global database of historic glacier lake outburst floods, Earth System Science Data, 15, 2983–3000, https://doi.org/10.5194/essd-15-2983-2023, 2023.
- Malakar, N. K., Hulley, G. C., Hook, S. J., Laraby, K., Cook, M., and Schott, J. R.: An Operational Land Surface Temperature Product for Landsat Thermal Data: Methodology and Validation, IEEE Transactions on Geoscience and Remote Sensing, 56, 5717–5735, https://doi.org/10.1109/TGRS.2018.2824828, 2018.
  - Mallalieu, J., Carrivick, J. L., Quincey, D. J., and Raby, C. L.: Ice-marginal lakes associated with enhanced recession of the Greenland Ice Sheet, Global and Planetary Change, 202, 103 503, https://doi.org/10.1016/j.gloplacha.2021.103503, 2021.
  - McFeeters, S. K.: The use of the Normalized Difference Water Index (NDWI) in the delineation of open water features, International Journal of Remote Sensing, 17, 1425–1432, https://doi.org/10.1080/01431169608948714, 1996.

- Melling, L., Leeson, A., McMillan, M., Maddalena, J., Bowling, J., Glen, E., Sandberg Sørensen, L., Winstrup, M., and Lørup Arildsen, R.: Evaluation of satellite methods for estimating supraglacial lake depth in southwest Greenland, The Cryosphere, 18, 543–558, https://doi.org/10.5194/tc-18-543-2024, 2024.
- Moon, T. A., Fisher, M., Stafford, T., and Thurber, A.: QGreenland (v3), National Snow and Ice Data Center, 500 https://doi.org/10.5281/zenodo.12823307, 2023.
  - Mouginot, J. and Rignot, E.: Glacier catchments/basins for the Greenland Ice Sheet, Dryad, https://doi.org/10.7280/D1WT11, 2019.
  - Naalakkersuisut: Impact Analysis of the Paris Agreement on Greenlandic Society, https://naalakkersuisut.gl/-/media/horinger/2023/02/0602\_parisaftale/eng-hovedrapport--konsekvensanalyse-af-parisaftalen-for-det-grnlandske-samfund.pdf, accessed: 2024-11-01, 2023.
- NASA Applied Remote Sensing Training (ARSET) program: ARSET Training: Satellite Remote Sensing for Measuring Urban Heat Islands and Constructing Heat Vulnerability Indices, https://code.earthengine.google.com/7103291d8b113cd38e573f2e3a67bb51, accessed: 2024-12-02, 2022.
  - Porter, C., Morin, P., Howat, I., Noh, M.-J., Bates, B., Peterman, K., Keesey, S., Schlenk, M., Gardiner, J., Tomko, K., Willis, M., Kelleher, C., Cloutier, M., Husby, E., Foga, S., Nakamura, H., Platson, M., Wethington, Michael, J., Williamson, C., Bauer, G., Enos, J., Arnold, G., Kramer, W., Becker, P., Doshi, A., D'Souza, C., Cummens, P., Laurier, F., and Bojesen, M.: ArcticDEM, Version 3, https://doi.org/10.7910/DVN/OHHUKH, 2018.
  - Ran, J., Ditmar, P., van den Broeke, M. R., Liu, L., Klees, R., Khan, S. A., Moon, T., Li, J., Bevis, M., Zhong, M., Fettweis, X., Liu, J., Noël, B., Shum, C. K., Chen, J., Jiang, L., and van Dam, T.: Vertical bedrock shifts reveal summer water storage in Greenland ice sheet, Nature, 635, 108–113, https://doi.org/10.1038/s41586-024-08096-3, 2024.

- Rick, B., McGrath, D., Armstrong, W., and McCoy, S. W.: Dam type and lake location characterize ice-marginal lake area change in Alaska and NW Canada between 1984 and 2019, The Cryosphere, 16, 297–314, https://doi.org/10.5194/tc-16-297-2022, 2022.
  - Rick, B., McGrath, D., McCoy, S. W., and Armstrong, W. H.: Unchanged frequency and decreasing magnitude of outbursts from ice-dammed lakes in Alaska, Nature Communications, 14, 6138, https://doi.org/10.1038/s41467-023-41794-6, 2023.
  - Röhl, K.: Thermo-erosional notch development at fresh-water-calving Tasman Glacier, New Zealand, Journal of Glaciology, 52, 203–213, https://doi.org/10.3189/172756506781828773, 2006.
- 520 Shugar, D. H., Burr, A., Haritashya, U. K., Kargel, J. S., Watson, C. S., Kennedy, M. C., Bevington, A. R., Betts, R. A., Harrison, S., and Strattman, K.: Rapid worldwide growth of glacial lakes since 1990, Nature Climate Change, 10, 939–945, https://doi.org/10.1038/s41558-020-0855-4, 2020.
  - St. Pierre, K. A., St. Louis, V. L., Schiff, S. L., and Sharp, M. J.: Proglacial freshwaters are significant and previously unrecognized sinks of atmospheric CO<sub>2</sub>, PNAS, 116, 17690–17695, https://doi.org/10.1073/pnas.1904241116, 2019.
- 525 Styrelsen for Dataforsyning og Infrastruktur: Sentinel2 10m 2022 mosaic. In: Satellitfoto Grønland, https://dataforsyningen.dk/data/4783, accessed: 2024-12-02, 2024.
  - Sutherland, J. L., Carrivick, J. L., Gandy, N., Shulmeister, J., Quincey, D. J., and Cornford, S. L.: Proglacial Lakes Control Glacier Geometry and Behavior During Recession, Geophysical Research Letters, 47, e2020GL088 865, https://doi.org/10.1029/2020GL088865, 2020.
  - Taylor, C., Robinson, T. R., Dunning, S., Carr, J. R., and Westoby, M.: Glacial lake outburst floods threaten millions globally, Nature Communications, 14, https://doi.org/10.1038/s41467-023-36033-x, 2023.

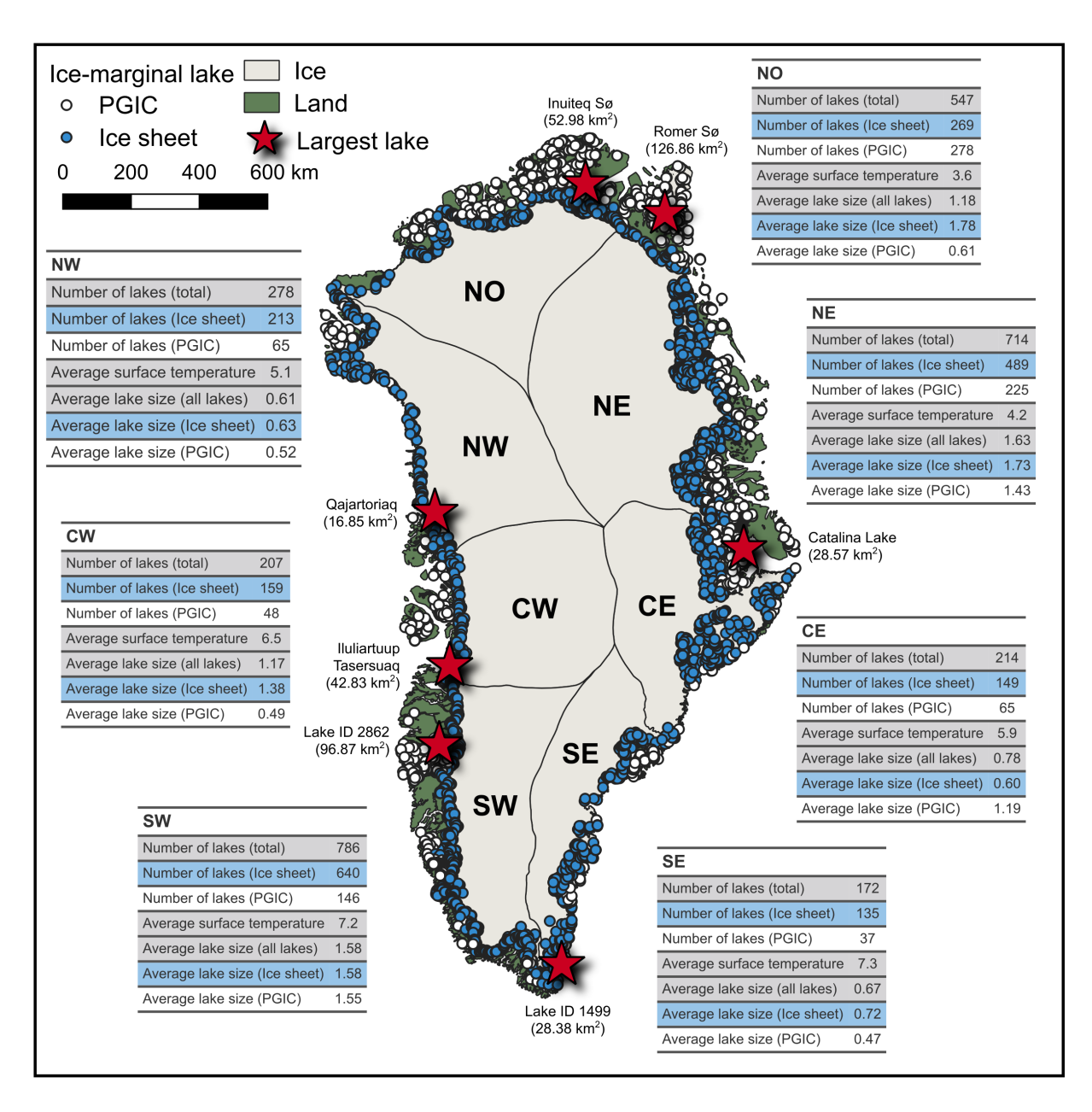
- Tomczyk, A. M., Ewertowski, M. W., and Carrivick, J. L.: Geomorphological impacts of a glacier lake outburst flood in the high arctic Zackenberg River, NE Greenland, Journal of Hydrology, 591, 125 300, https://doi.org/10.1016/j.jhydrol.2020.125300, 2020.
- Urbański, J. A.: Monitoring and classification of high Arctic lakes in the Svalbard Islands using remote sensing, International Journal of Applied Earth Observation and Geoinformation, 112, 102 911, https://doi.org/https://doi.org/10.1016/j.jag.2022.102911, 2022.
- U.S. Geological Survey: Landsat Atmospheric Auxiliary Data Data Format Control Book (DFCB) version 6.0, Department of the Interior U.S. Geological Survey, https://d9-wret.s3.us-west-2.amazonaws.com/assets/palladium/production/s3fs-public/media/files/LSDS-1329\_ Landsat-Atmospheric-Auxiliary DFCB v6.pdf, 2023.
  - Veh, G., Lützow, N., Tamm, J., Luna, L. V., Hugonnet, R., Vogel, K., Geertsema, M., Clague, J. J., and Korup, O.: Less extreme and earlier outbursts of ice-dammed lakes since 1900, Nature, 614, 701–707, https://doi.org/10.1038/s41586-022-05642-9, 2023.
- Veh, G., Wang, B. G., Zirzow, A., Schmidt, C., Lützow, N., Steppat, F., Zhang, G., Vogel, K., Geertsema, M., Clague, J. J., and Korup, O.: Progressively smaller glacier lake outburst floods despite worldwide growth in lake area, Nature Water, 3, 271–283, https://doi.org/10.1038/s44221-025-00388-w, 2025.
  - Wang, S., Li, J., Zhang, W., Cao, C., Zhang, F., Shen, Q., Zhang, X., and Zhang, B.: A dataset of remote-sensed Forel-Ule Index for global inland waters during 2000–2018, Scientific Data, 8, https://doi.org/10.1038/s41597-021-00807-z, 2021.
- Warren, C. R. and Kirkbride, M. P.: Calving speed and climatic sensitivity of New Zealand lake-calving glaciers, Annals of Glaciology, 36, 173–178, https://doi.org/10.3189/172756403781816446, 2003.
  - Wieczorek, I., Strzelecki, M. C., Stachnik, Ł., Yde, J. C., and Małecki, J.: Post-Little Ice Age glacial lake evolution in Svalbard: inventory of lake changes and lake types, Journal of Glaciology, 69, 1449–1465, https://doi.org/10.1017/jog.2023.34, 2023.
- Wiesmann, A., Santoro, M., Caduff, R., How, P., Messerli, A., Mätzler, E., Langley, K., Høegh Bojesen, M., Paul, F., and Kääb, A. M.: ESA

  Glaciers Climate Change Initiative (Glaciers\_cci): 2017 inventory of ice marginal lakes in Greenland (IIML), v1, Centre for Environmental

  Data Analysis, https://doi.org/10.5285/7ea7540135f441369716ef867d217519, 2021.

- Wilkinson, M. D., Dumontier, M., Aalbersberg, I. J., Appleton, G., Axton, M., Baak, A., Blomberg, N., Boiten, J.-W., da Silva Santos, L. B., Bourne, P. E., Bouwman, J., Brookes, A. J., Clark, T., Crosas, M., Dillo, I., Dumon, O., Edmunds, S., Evelo, C. T., Finkers, R., Gonzalez-Beltran, A., Gray, A. J., Groth, P., Goble, C., Grethe, J. S., Heringa, J., 't Hoen, P. A., Hooft, R., Kuhn, T., Kok, R., Kok, J., Lusher, S. J.,
  Martone, M. E., Mons, A., Packer, A. L., Persson, B., Rocca-Serra, P., Roos, M., van Schaik, R., Sansone, S.-A., Schultes, E., Sengstag, T., Slater, T., Strawn, G., Swertz, M. A., Thompson, M., van der Lei, J., van Mulligen, E., Velterop, J., Waagmeester, A., Wittenburg, P., Wolstencroft, K., Zhao, J., and Mons, B.: The FAIR Guiding Principles for scientific data management and stewardship, Scientific Data, 3, 2052–4463, https://doi.org/10.1038/sdata.2016.18, 2016.
- Winstrup, M., Ranndal, H., Hillerup Larsen, S., Simonsen, S. B., Mankoff, K. D., Fausto, R. S., and Sandberg Sørensen, L.: PRODEM: an annual series of summer DEMs (2019 through 2022) of the marginal areas of the Greenland Ice Sheet, Earth System Science Data, 16, 5405–5428, https://doi.org/10.5194/essd-16-5405-2024, 2024.
  - Xu, H.: Modification of normalised difference water index (NDWI) to enhance open water features in remotely sensed imagery, International Journal of Remote Sensing, 27, 3025–3033, https://doi.org/10.1080/01431160600589179, 2006.
  - Zhang, E., Catania, G., and Trugman, D. T.: AutoTerm: an automated pipeline for glacier terminus extraction using machine learning and a "big data" repository of Greenland glacier termini, The Cryosphere, 17, 3485–3503, https://doi.org/10.5194/tc-17-3485-2023, 2023a.

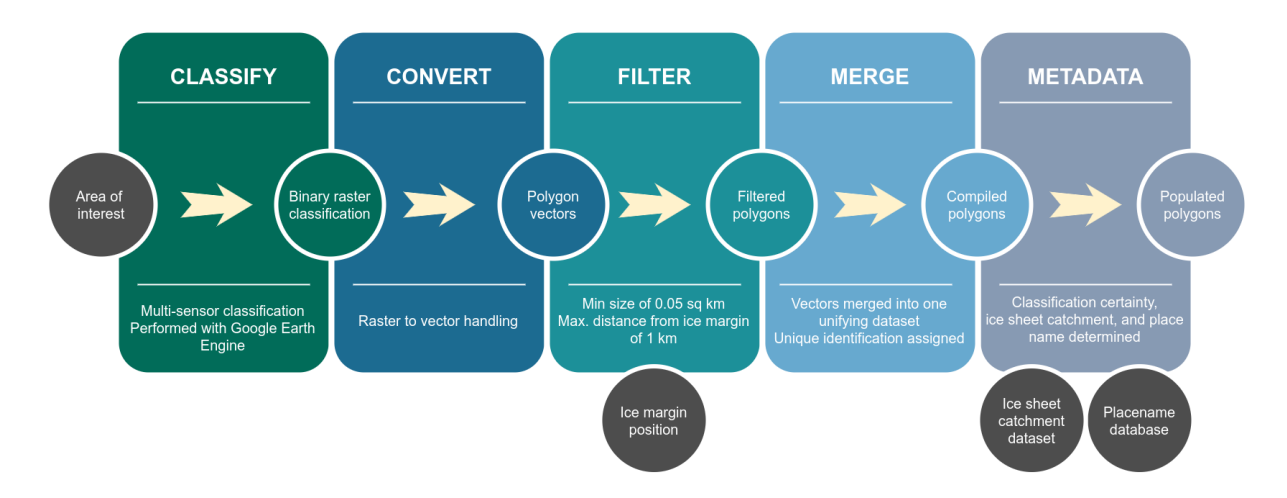
- Zhang, G., Bolch, T., Yao, T., Rounce, D., Chen, W., Veh, G., King, O., Allen, S. K., Wang, M., and Wang, W.: Underestimated mass loss from lake-terminating glaciers in the greater Himalaya, Nature Geoscience, 16, 333–338, https://doi.org/10.1038/s41561-023-01150-1, 2023b.
- Zhang, G., Carrivick, J. L., Emmer, A., Shugar, D. H., Veh, G., Wang, X., Labedz, C., Mergili, M., Mølg, N., Huss, M., Allen, S., Sugiyama,
  S., and Lützow, N.: Characteristics and changes of glacial lakes and outburst floods, Nature Reviews Earth and Environment, 5, 447–462,
  https://doi.org/10.1038/s43017-024-00554-w, 2024.



**Figure 1.** An overview of the abundance of lakes in ice-marginal lake inventory series, 2016-2023. Each mapped point denotes a unique lake, mapped across the Greenland Ice Sheet margin (blue) and the surrounding PGIC margins (white). The tables associated with each region present general statistics (with average surface temperature values provided in degrees Celsius). Red starred points on the map correspond to the largest lake of each region, with placenames sourced from the placename database provided by Oqaasileriffik (the Language Secretariat of Greenland) and inventory identification numbers presented where a name is not given. It is noted that the name of the largest lake in the CE region (Catalina Lake) is not present in the placename database, and instead we adopt the lake name from Grinsted et al. (2017). The catchment regions are those defined by Mouginot and Rignot (2019). Base maps for plotting are from QGreenland v3.0 (Moon et al., 2023).

Table 2. Summary of metadata included with each ice-marginal lake inventory in the annual series

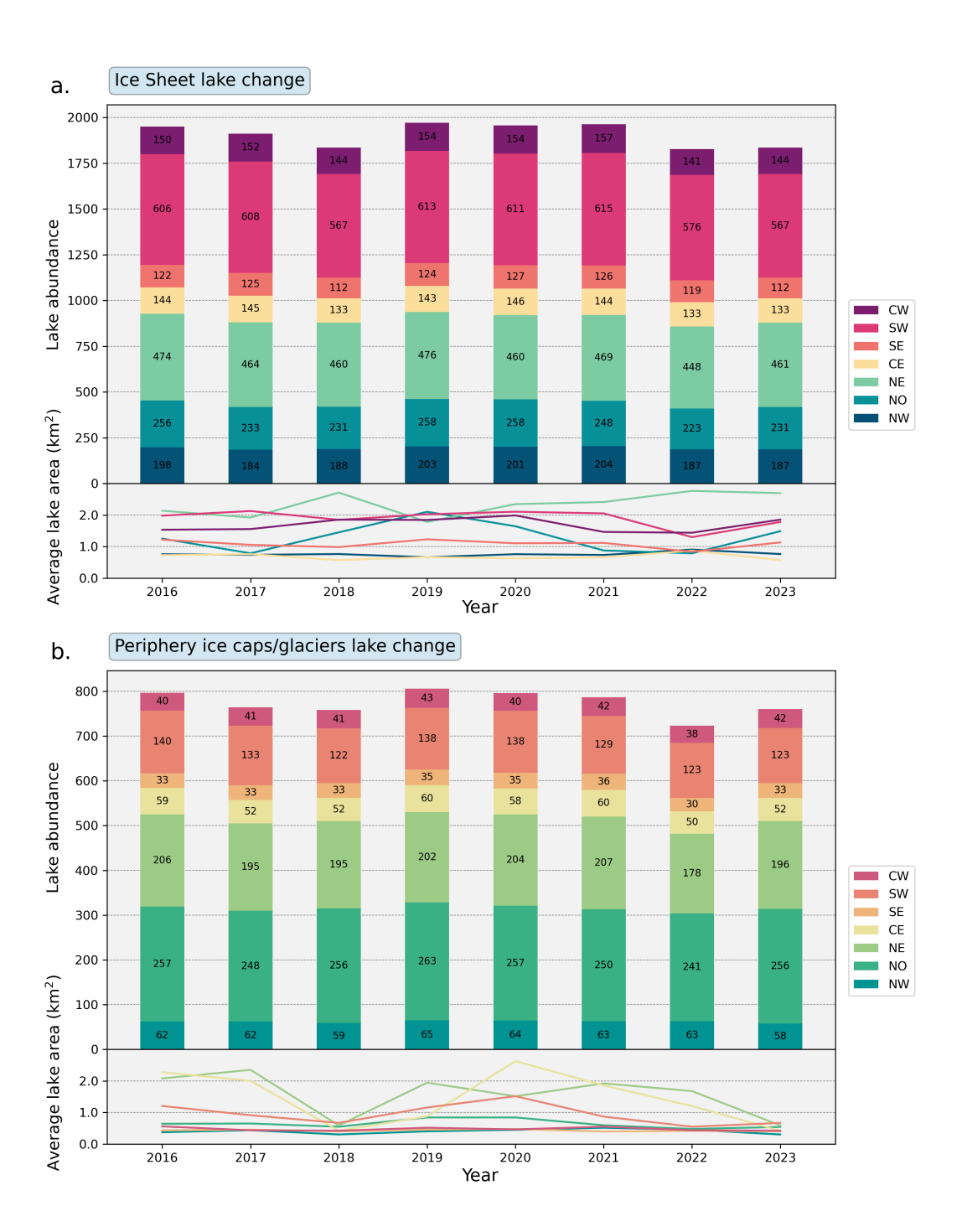
Variable name	Description	Format
lake_id	Identifying number for each unique lake	Integer
lake_name	Lake placename, as defined by the placename database provided by Oqaasileriffik (the Lan-	
	guage Secretariat of Greenland) (https://nunataqqi.gl/) which is distributed with QGreenland	
	(https://qgreenland.org/). If no lake name is given then the placename is classed as "Unknown".	
margin	Type of margin that the lake is adjacent to ("ICE_SHEET", "ICE_CAP")	String
region	Region that lake is located, as defined by Mouginot and Rignot (2019) ("NW", "NO", "NE", "CE", "SE", "SW", "CW")	String
area_sqkm	Areal extent of polygon/s in square kilometres	Float
length_km	Length of polygon/s perimeter in kilometres	Float
centroid	Centroid position (x,y) of lake, based on all classifications throughout the inventory series.	String
	Coordinates are provided in the WGS NSIDC Sea Ice Polar Stereographic North (EPSG:3413) projected coordinate system	
temp_aver	Average lake surface temperature estimate for the month of August (in degrees Celsius), derived	Float
	from the Landsat 8/9 OLI/TIRS Collection 2 Level 2 surface temperature data product	
temp_min	Minimum pixel lake surface temperature estimate for the month of August (in degrees Celsius),	Float
	derived from the Landsat 8/9 OLI/TIRS Collection 2 Level 2 surface temperature data product	
temp_max	Maximum pixel lake surface temperature estimate for the month of August (in degrees Celsius),	Float
	derived from the Landsat 8/9 OLI/TIRS Collection 2 Level 2 surface temperature data product	
temp_stdev	Average lake surface temperature estimate standard deviation for the month of August, derived	Float
	from the Landsat 8/9 OLI/TIRS Collection 2 Level 2 surface temperature data product	
temp_count	Number of Landsat 8/9 OLI/TIRS Collection 2 Level 2 scenes that lake surface temperature	Integer
	information were derived from. Scenes are only selected from the month of August	
temp_date	Date and time of all Landsat 8/9 OLI/TIRS Collection 2 Level 2 scene acquisitions that lake	String
	surface temperature information are derived from	
method	Method of classification ("DEM", "SAR", "VIS")	String
source	Image source of classification ("ARCTICDEM", "S1", "S2")	String
all_src	List of all sources that successfully classified the lake (i.e. all classifications with the same "lake_name" value)	String
num_src	Number of sources that successfully classified the lake ("1", "2", "3")	Integer
certainty	Certainty of classification, which is calculated from "all_src" as a score between "0" and "1"	Float
start_date	Start date for classification image filtering	String
end_date	End date for classification image filtering	String
verified	Flag to denote if the lake has been manually verified ("Yes", "No")	String
verif_by	Author of verification	String
edited	Flag to denote if polygon has been manually edited ("Yes", "No")	String
edited_by	Author of manual editing	String



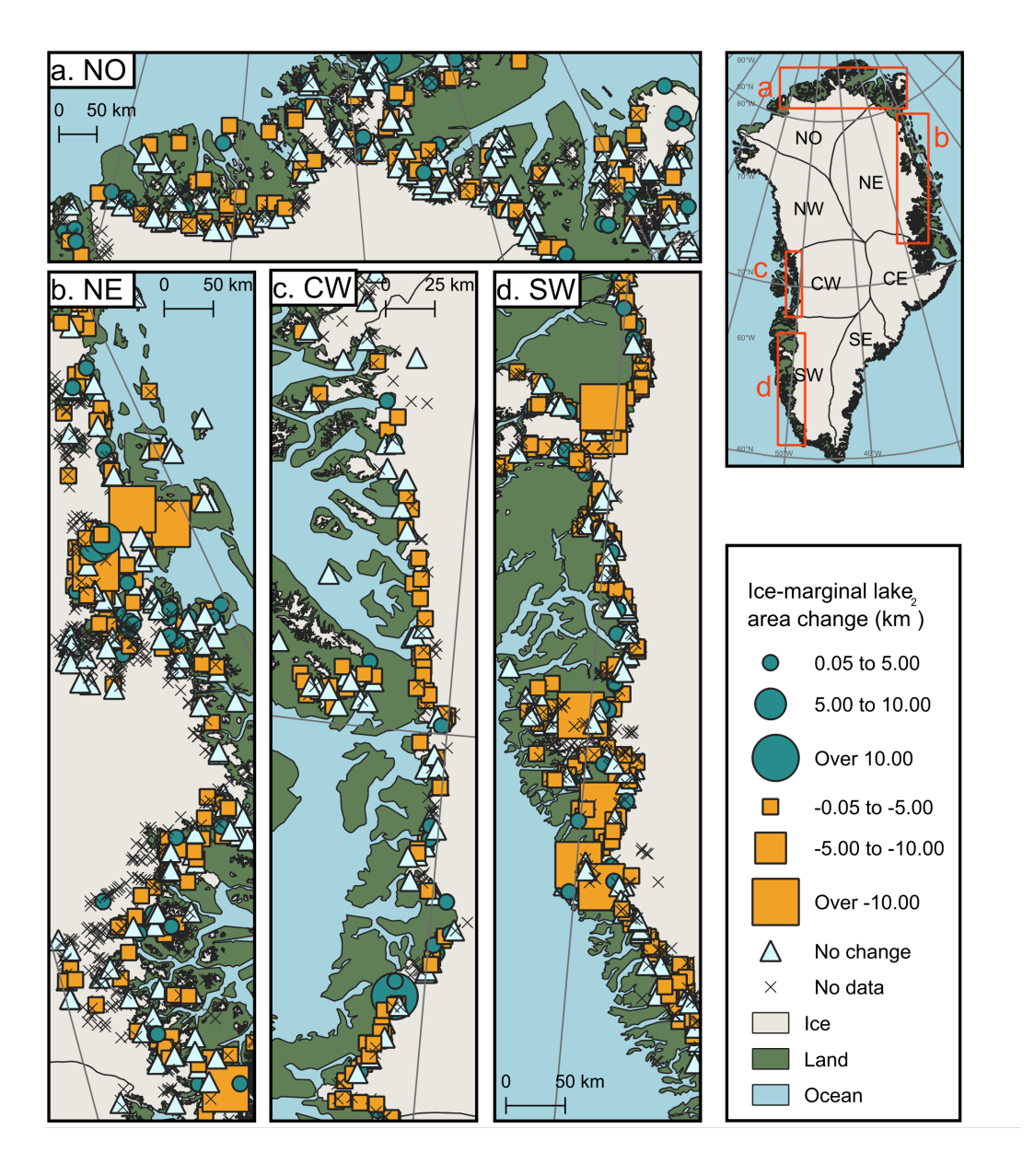
**Figure 2.** A visualisation of the processing workflow for the generation of the ice-marginal lake inventory series, including components performed with Google Earth Engine ("Classify") and the Python package GrIML (How, 2024), which utilises Python spatial data handling packages geopandas (Kelsey et al., 2020) and rasterio (Gillies et al., 2013–). The workflow is based on How et al. (2021). The annotated rectangles refer to process stages (reading from left to right), the coloured annotated circles represent intermediary outputs to the corresponding process stages in the workflow, and the grey annotated circles represent workflow inputs.

Table 3. Summary of multi-spectral indices for ice-marginal lake classification from Sentinel-2 Level 1C scenes

Spectral index	Equation	Threshold/s	Target
Normalised Difference	$(B3 - B8) \div (B3 + B8)$	< 0.3	Open water with shadowing
Water Index (NDWI)			
Modified Normalised	$(B3 - B11) \div (B3 + B11)$	> 0.1	Snow/ice in water
Difference Index			
(MNDWI)			
Automated Water Ex-	$B2+2.5\times B3-1.5\times (B8+B11)-0.25\times B12$	> 2000 & < 5000	Optimised sediment-loaded
traction Index (with			water without shadowing
shadow) (AWEIsh)			
Automated Water	$4\times ({\rm B3-B11}) - (0.25\times {\rm B8} + 2.75\times {\rm B12})$	> 4000 & < 6000	Sediment-loaded water with
Extraction Index (no			shadowing
shadow) (AWEInsh)			
Snow Brightness Ratio	$(B4 + B3 + B2) \div 3$	< 5000	Snow-covered areas
(BRIGHTNESS)			



**Figure 3.** Change in the abundance and average area (km<sup>2</sup>) of ice-marginal lakes around the ice sheet margin (a) and PGIC margins (b). Each of the coloured bars denote lake abundance per region for a given year of the inventory series (2016-2023), with annotated numbers corresponding to the number of lakes classified for each region. Each line plot indicates the average lake area per region for a given year of the inventory series. Average lake area is compiled from all lakes classified from SAR and multi-spectral imagery, as DEM classifications are not a direct detection of water bodies.



**Figure 4.** Change in lake area across the ice-marginal lake inventory series, 2016-2023. Example regions are highlighted from NO (a), NE (b), CW (c), and SW (d) regions of both the ice sheet and the PGICs. Lake area increase (purple circles), lake area decrease (yellow squares), and unchanged lake areas (white triangles) are mapped, with the size of the symbol denoting the amplitude of change (km<sup>2</sup>). Each point denotes the change in lake size across the inventory series, as classified using the SAR and multi-spectral imagery methods. Lakes with no available area data (i.e. not classified using the SAR and multi-spectral imagery methods) are marked with crosshairs. The catchment regions are those defined by Mouginot and Rignot (2019). Base maps for plotting are from QGreenland v3.0 (Moon et al., 2023).

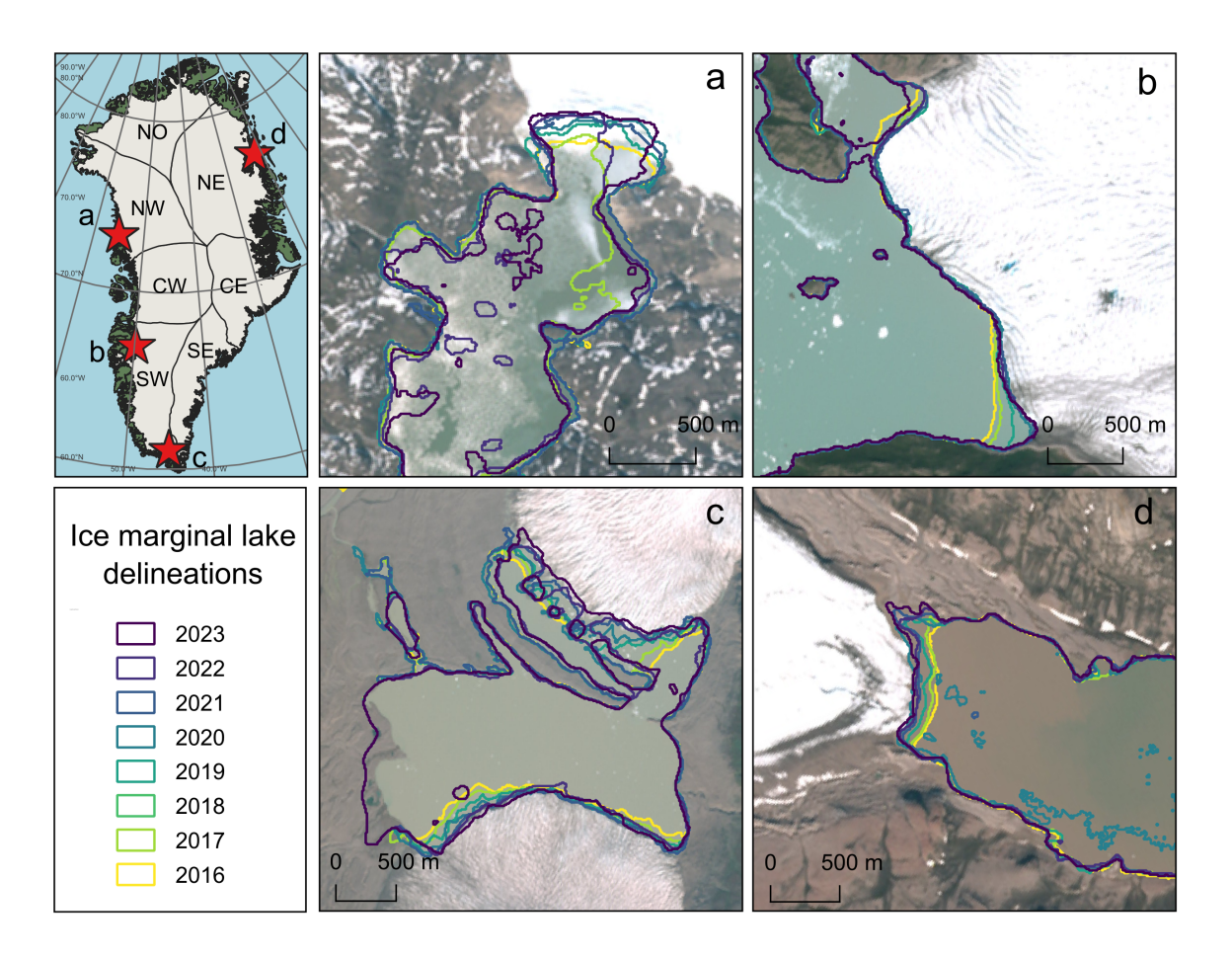


**Figure 5.** Examples of lake morphology change, and the corresponding evolution of ice termini morphology, from the ice-marginal lake inventory series. These examples highlight basin margin retreat (a), peripheral margin retreat (b), bilateral margin retreat (c), and focused margin retreat (d). It is noted that the example from (a) is a lake with persistent ice cover throughout the summer season. The background satellite imagery presented is from a Sentinel-2 10 m 2022 mosaic (Styrelsen for Dataforsyning og Infrastruktur, 2024). The base layers for the insert map plotting are from QGreenland v3.0 (Moon et al., 2023).

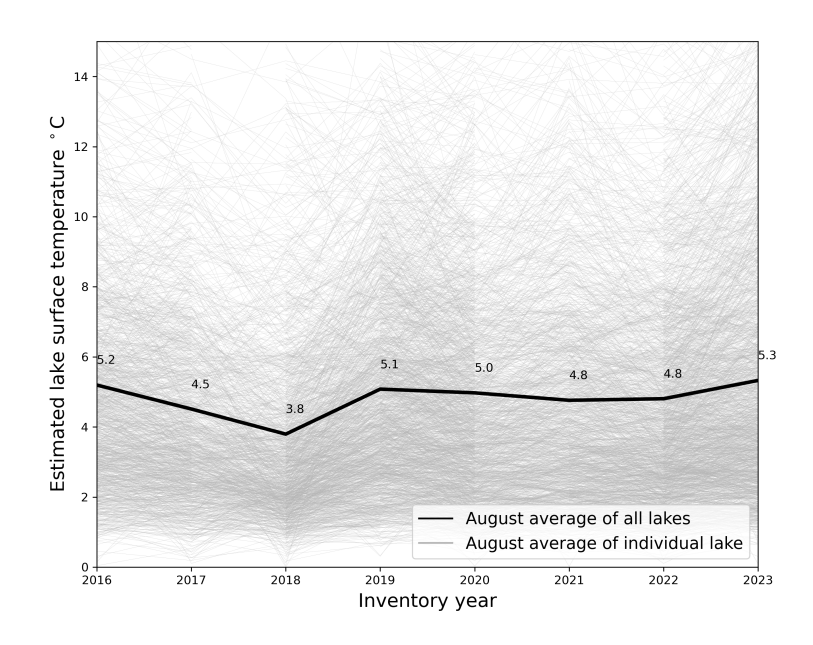


**Figure 6.** Average lake surface temperature estimates from the month of August at each inventory lake for each inventory year (2016-2023) (grey). The average of all lakes (black) is the sum of all lake averages divided by the number of lakes. Lake surface temperature is derived from Landsat 8 and Landsat 9 OLI/TIRS Collection 2 Level 2 surface temperature data product. Averages are calculated from all available scenes acquired from the month of August to limit the risk of mis-estimates due to ice-covered conditions, with all estimates below 0°C removed.

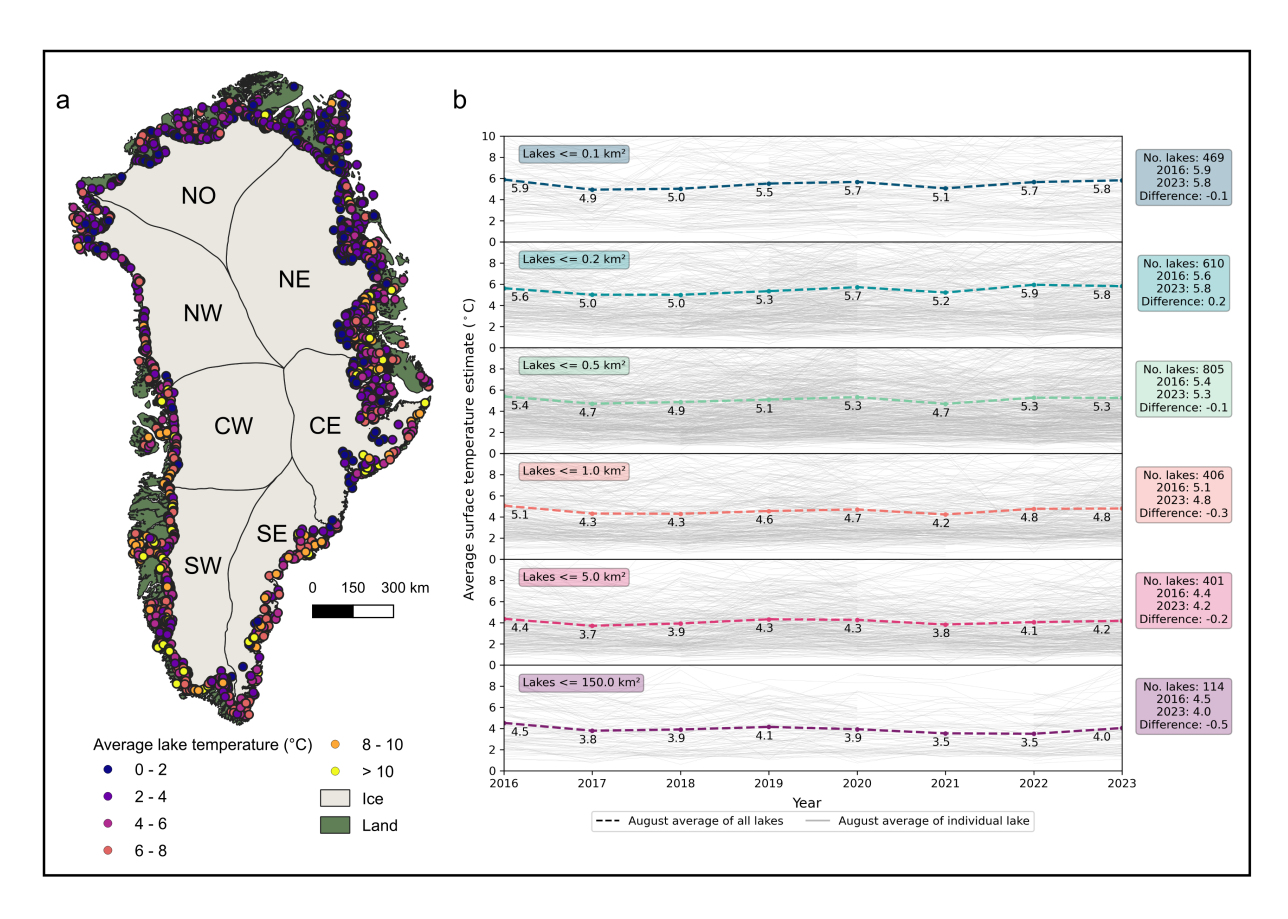


**Figure 7.** Spatial and temporal evolution of average lake surface temperature estimates at each inventory lake. Lake surface temperature estimates for each ice-marginal lake are represented by colour in (a), where a surface temperature estimate for each lake is the average value across all inventory years. The temporal variability in lake surface temperature estimate is shown in (b), divided by lake size across six size groups. Individual lake temperature estimates (grey) are overlain by the average of all lakes within each size group (black) (i.e. the sum of all lake averages in each group divided by the number of lakes). All estimates below 0°C are removed. The base map for plotting is from QGreenland v3.0 (Moon et al., 2023), with catchment regions as defined by Mouginot and Rignot (2019).

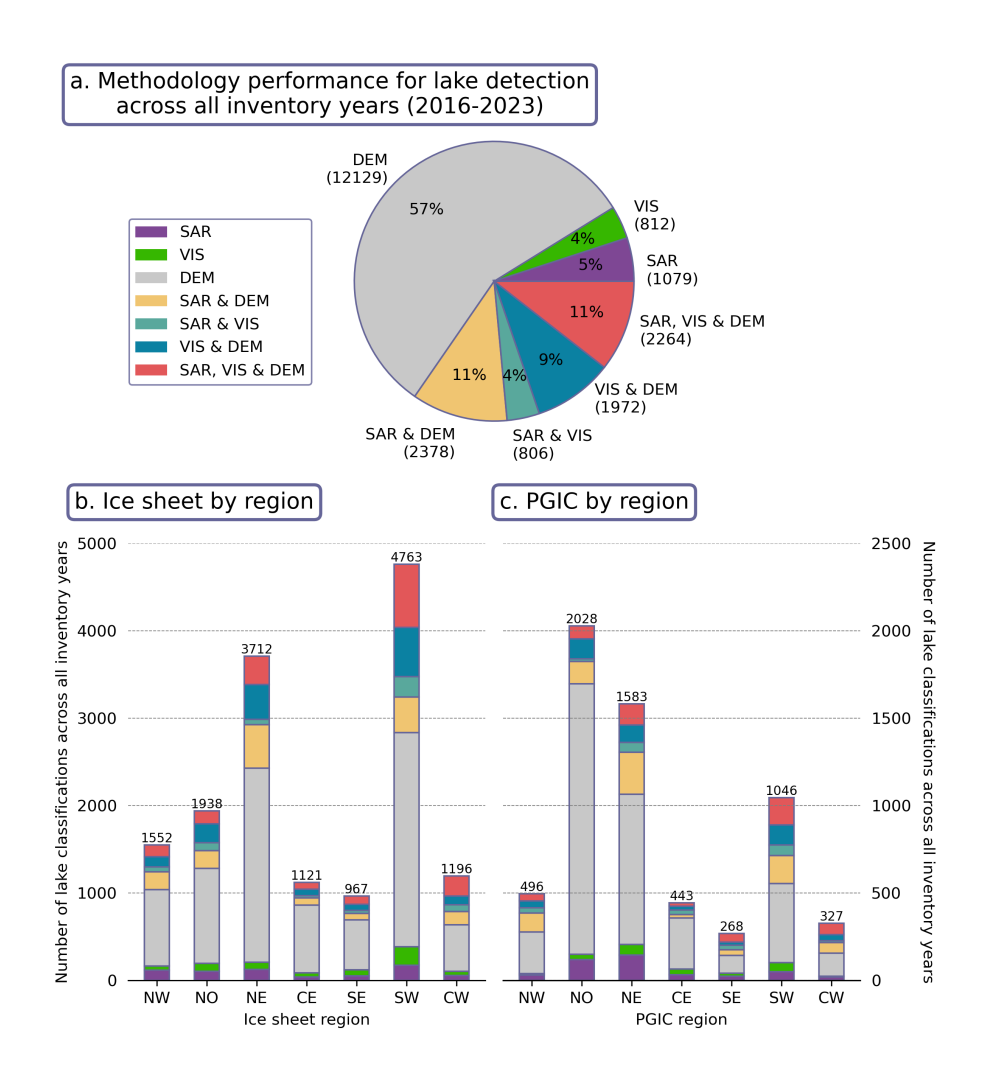


**Figure 8.** Lake classifications by method across the ice-marginal lake inventory series, with an overview of lake classifications over all inventory years (a) and classifications by region for lakes adjacent to the ice sheet (b) and the PGICs (c). SAR refers to the SAR backscatter classification method from Sentinel-1 imagery, VIS refers to the multi-spectral classification method from Sentinel-2 imagery, DEM refers to the DEM sink detection method from the ArcticDEM, and listed methods refer to instances where more than one method has been used to classify a lake (e.g. "SAR & DEM", "SAR, VIS & DEM"). The legend and colour scheme in (a) correspond to (b) and (c). Values in brackets in (a) are the absolute number of lakes corresponding to the provided percentages. The values printed on top of the bars in (b) are the total number of classifications in the given region.

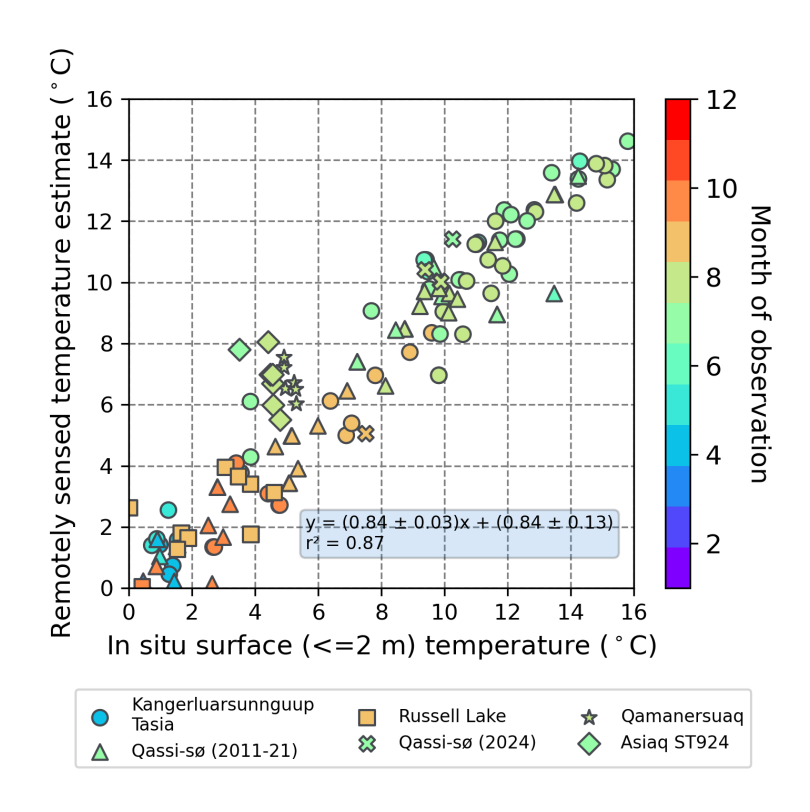


**Figure 9.** Comparison of in situ surface (<= 2 m) water temperature measurements with remotely sensed temperature estimates (°C) from Kangerluarsunnguup Tasia (circle), Qassi-Sø (2011-21) (triangle), Russell Lake (square), Qassi-Sø (2024) (cross), Qamanersuaq (star) and Asiaq station 924 (ST924) (diamond). The colour of each point corresponds to the month that the observation was collected. All observations are from afternoon acquisitions (between 13.00-15.00 UTC).